

On the incompressibility of cylindrical origami patterns

Friedrich Bös,¹ Etienne Vouga,² Omer Gottesman,³ and Max Wardetzky¹

¹*Institute for Numerics and Applied Mathematics,*

University of Göttingen, 37083 Göttingen, Germany

²*Department of Computer Science, The University of Texas at Austin, Austin, Texas 78712, USA*

³*School of Engineering and Applied Sciences,*

Harvard University, Cambridge, Massachusetts 02138, USA

(Dated: June 21, 2022)

We investigate the axial compressibility of origami cylinders, i.e., cylindrical structures folded from rectangular sheets of paper. We prove, using geometric arguments, that a general fold pattern only allows for a finite number of *isometric* cylindrical embeddings. Therefore, compressibility of such structures requires stretching the material or deforming the folds. Our result complements the celebrated "bellows theorem" and extends it to the setting of cylindrical origami whose top and bottom are not necessarily rigid, and severely restricts the space of constructions that must be searched when designing new types of origami-based rigid-foldable deployable structures and metamaterials.



Figure 1: Compressing an origami cylinder made from ordinary paper suggests that it can rigidly collapse. But is this indeed so?

INTRODUCTION

The art and science of folding intricate three dimensional structures out of thin materials, such as paper, has occupied artists, designers, engineers, and mathematicians for decades. More recently, origami-like structures have found their way into designing deployable structures [1] and mechanical metamaterials [2]. While considerable effort has been put into studying collapsible, or rigid-foldable,

origami [3], various questions about global rigidity and *flexibility* still remain poorly understood. Consider the problem of crushing a coke can: axially compressing a thin cylinder. It has long been known that (i) such compression results in diamond-shaped (Yoshimura) crease patterns [4, 5] and (ii) crushing an ideal cylinder unavoidably induces in-plane stress in the cylinder. On the other hand, there exist numerous examples of origami-type cylinders that *appear* to be truly rigidly foldable—

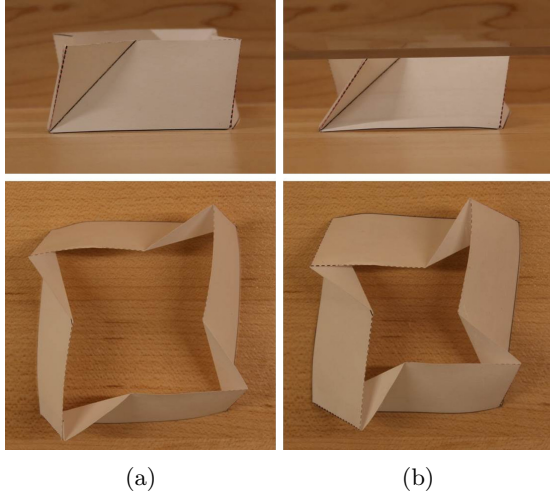


Figure 2: A fold pattern to which the bellows theorem does not apply. Its apparent collapsibility is disproven by our result.

deformable purely isometrically, without any in-plane strain; see the figure above and the supplemental video. But is this really so?

The work of Guest and Pellegrino [6] informs us that purely isometric deformations are indeed possible *if* one allows for sliding of folds within the material, which, however, cannot be considered origami-type foldability. Recently, Yasuda and Yang [7] have constructed fold pattern for origami-type cylinders that allow for true rigid foldability *without* moving folds within the material. In this letter, we show that in general most such fold patterns cannot be isometrically compressed axially, and the apparent foldability of such structures requires bending or stretching the flat origami pieces. This work can thus guide the design of foldable origami patterns.

We formulate the problem of rigid foldability as a root finding problem for a certain *real analytic* function (to be specified below) of the cylinder's compression ratio. We show that this function has at least one nonzero value, implying that it can only have isolated zeros, which rules out continuous isometric deformations.

The study of rigid foldability for closed surfaces, i.e., two-dimensional structures without holes, has a long tradition in mathematics. For instance, Cauchy's theorem [8, 9] asserts that the boundary surface of a convex body is always rigid; moreover, the famous *bellows theorem* [10] states that a flexible closed surface must maintain its enclosed volume during isometric deformation. Applied to the problem of foldable origami-type cylinders, the bellows theorem rules out rigid foldability *provided* that the cylinders' top and bottom do not alter shape when being deformed (since then the cylinder could be sealed with end caps to form a closed surface, as is the case for the example shown in Fig. 1). The proof of the bellows theorem is, however, quite involved mathematically. Our result extends the bellows theorem by proving that it is impossible to crush a large class of origami-type cylinders (e.g., those shown in Fig. 2) without the restricting assumption that the cylinders's top and bottom maintain their shape during deformation.

ORIGAMI CYLINDERS

We define a fold pattern in the (uv) -plane as a finite set of straight *fold lines* drawn on a rectangular strip of dimensions $l \times h$. We define *origami cylinders* as isometric embeddings of such fold pattern into 3D (xyz) -space, such that (i) fold lines are mapped to straight line segments, (ii) the embedding is piecewise C^4 [11], and (iii) all horizontal lines in the material domain map to closed curves lying in planes perpendicular to the z -axis.

Using these definitions, we formalize our question as: does there exist a *fixed* fold pattern and a corresponding one-parameter family of origami cylinders of continuously varying axial height? To answer this question, we consider a decomposition of the material domain into *strips*. Let *vertices* be those points where fold lines cross each other or the boundary. Strips arise from cutting along the horizonta-

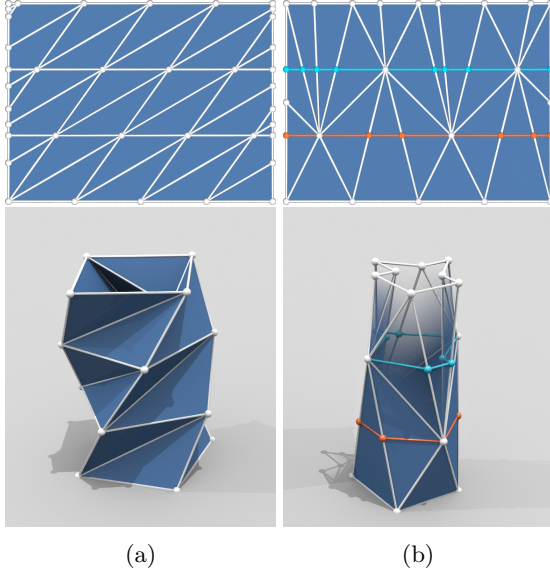


Figure 3: Two origami cylinders with regular (a) and irregular (b) fold patterns (white lines) and illustration of strip construction (blue and orange lines).

tal lines passing through each of the pattern’s vertices, followed by splitting any fold line that intersects such a horizontal line into two pieces and adding an auxiliary vertex between them; see Fig. 3b. We reduce the question of isometric compressibility of origami cylinders to the question of compressing the embeddings of individual strips.

Fold lines decompose each strip into triangles and quadrilaterals that extend from the strip’s top to its bottom. Our requirements (i)-(iii) above imply that the embeddings of these triangles and quadrilaterals must be flat: *Every origami cylinder whose height is strictly less than the material height consists entirely of planar facets.* In particular, all triangles and quads within each embedded strip are then planar. Notice that, while this result may seem intuitively clear, our assumptions only require straight embedded fold lines but do not explicitly impose conditions on the surface in be-

tween. We refer to the supplementary material for a proof of these statements.

FAN CONSTRUCTION

Each strip consists of planar triangles and quadrilaterals. By inserting an arbitrary auxiliary diagonal per quad (which may be viewed as an extra fold line that can only *increase* but not decrease a strip’s flexibility), strips can be decomposed into a collection of *fans*. A fan is a *maximal* subset of the material that is bounded between fold lines that emanate from a common vertex, see Fig. 3. We call a fan *downward*, if the respective vertex lies on the top of the strip; otherwise, we call it *upward*. Notice that downward and upward fans alternate and that two consecutive fans share a common fold line. We call the two outermost fold lines and vertices of a fan *exterior*, the others *interior*.

We now study the embedding of a single strip of material height h into space, relaxing the condition that the strip is closed, i.e., the left and right boundaries of the strip do not have to coincide in space. Let H denote the strip’s embedded height. If $H < h$, then up to rigid motions, there are at most finitely many isometric embeddings, and they can be constructed using a straightforward procedure. To see this, we first show that a single downward fan with n bottom vertices has at most 2^{n-1} distinct isometric embeddings. Let a be the apex of the fan in the material domain and let A be its embedded position on the $z = H$ plane, so that the fan’s bottom boundary must embed in the (xy) -plane. Label the exterior vertices of the fan in the material domain p_1 and p_n . Suppose that the embedded position P_1 of p_1 is given, with $|P_1A| = |p_1a|$. We now embed the remaining bottom vertices p_2, p_3, \dots, p_n in the order they appear along the material boundary. In order to construct the position P_2 of p_2 , note that P_2 has to satisfy three length constraints: one to P_1 , one to A , and one to P_3 , which has not yet been placed. The first two conditions, along

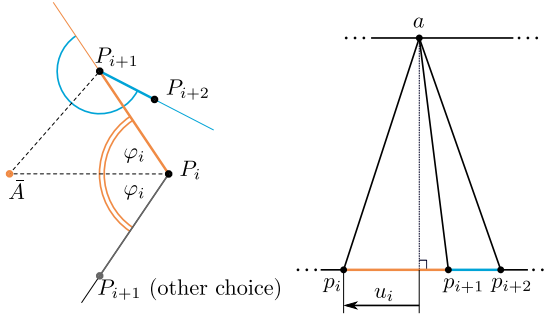


Figure 4: Illustration of the ray construction. *Left:* embedded space (top view); *right:* material domain. Here u_i is the signed horizontal distance from a to p_i (i.e., in this case, $u_i < 0$).

with the fact that P_2 must lie in the (xy) -plane, are enough to determine (two possible positions of) P_2 while the third will be used to determine P_3 , and so on.

To see this, denote by \bar{A} the vertical projection of A onto the (xy) -plane. Then the angle $\varphi_i = \angle \bar{A} P_i P_{i+1}$ satisfies

$$\cos(\varphi_i) = \frac{-u_i}{\sqrt{h^2 - H^2 + u_i^2}}, \quad (1)$$

where u_i is the signed horizontal distance in the material from a to p_i , see Fig. 4. In other words, once P_i is constructed, the embedded point P_{i+1} must lie on one of two rays originating at P_i and symmetric about $P_i \bar{A}$, where angles can be found using (1). Once a ray is chosen along which P_{i+1} must lie, the precise position along the ray is given by requiring that $|P_i P_{i+1}| = |p_i p_{i+1}|$. A proof of (1) can be found in the supplemental material. Note also that Eq. 1 implies that vertical folds (with $u_i = 0$) must have dihedral angle $\pm\pi$ whenever $H < h$.

Since there are two choices for where to place each P_i for $2 \leq i \leq n$, there are at most 2^{n-1} possible embeddings (disregarding self-penetration). There is another observation to be made: since fold lines with zero dihedral angle necessarily give rise to an isometric embedding, it follows that during the ray construction

process, one of the two rays originating from P_{i+1} on which P_{i+2} resides must lie on the line connecting P_{i+1} with P_i , see Fig. 4. It follows that of all possible embeddings, only two are “nondegenerate” in that they have no fold lines with zero dihedral angle (one for each choice of P_2).

A perfectly analogous argument shows that an upward fan with n top vertices can be embedded in at most 2^{n-1} ways, given an embedding of its left boundary. Finally, this construction shows that the entire strip can be embedded in finitely many ways, given an embedding of the strip’s leftmost boundary (which determines the rigid motion), by marching from left to right across the strip.

The above construction provides a necessary condition for whether a given fold pattern embeds as an origami cylinder: consider all of the embeddings of each individual strip and check if any of them close up.

CYLINDER COMPRESSION

Using the notation and results established above, we show that a large class of origami cylinders *cannot* be compressed isometrically. In particular, our results prove that the fold patterns considered by Yasuda and Yang [7] are one of the very few patterns that allow for rigid foldability: *Given a fold pattern, the origami cylinders folded from that pattern can attain only a finite set of embedded heights, provided that there is no strip that contains a vertical fold line. Each strip with vertical fold lines must either be embedded with $H = h$ or its vertical creases must have dihedral angles of $\pm\pi$.* Consequently, there does not exist a family of valid embeddings whose heights decrease continuously—the cylinder cannot be folded rigidly.

To see this, we show that the statement holds for a single strip that contains no vertical fold line. Choose coordinates so that the top-left corner $(0, h)$ of the strip’s material do-

main embeds at $(0, 0, H)$ and the bottom-left corner $(0, 0)$ embeds at $C_1 = (\lambda, 0, 0)$, where $\lambda = \sqrt{h^2 - H^2}$ is an increasing function of the compression ratio. Now recall that for a given fold pattern, each of the finitely many *open* strip embeddings can be encoded by the choices of the signs of the angles φ in (1). Given such a choice of signs, the position of the embedded bottom-right corner, C_2 , is uniquely determined. A necessary condition for the embedded strip being closed is that $C_1 = C_2$; one measure of the failure of the strip to close up is the *gap* $|C_2 - C_1|^2$.

The key observation is that for every fixed choice of signs, the gap g is a *real analytic* function of the embedded height, H . Indeed, g is a function of the fixed material dimensions and the angles φ , which are analytic in H . The precise form of g is given in the supplemental material. Valid embedding heights H are a subset of the zeros of the functions g . Now consider the special case $H = h$. In this case, property (iii) together with the assumption that the strip has no vertical fold line imply that the only possible embedding of the strip is the rigid one, e.g., the embedding of the material as a flat rectangle of size $l \times h$ perpendicular to the (xy) -plane. It follows that $g(h) = l \neq 0$. Since g is real analytic and not identically zero, its roots must be finite and isolated, proving the statement.

SUMMARY

We have investigated the compressibility of cylindrical origami structures and have shown that in general such structures cannot be compressed isometrically. The fact that structures such as those presented in Fig. 1 and Fig. 2 appear to be isometrically compressible suggests that the requisite stretching is localized to specific regions—to the effect that macroscopic deformations of the material remain small. The principles leading to such localized stretching and their applicability to the design of foldable origami will be subject of future work.

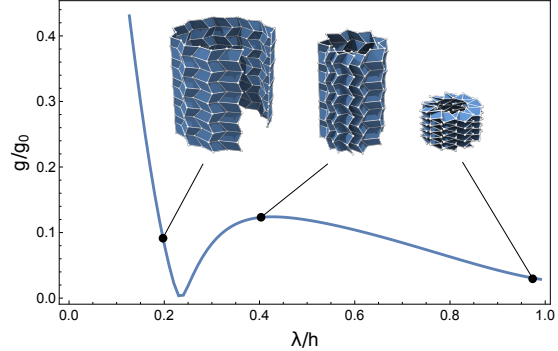


Figure 5: Plot of normalized gap magnitude as a cylindrical Miura pattern is compressed. We prove this function vanishes at only finitely many values of λ , and so the pattern is not rigid-foldable.

ACKNOWLEDGEMENTS

F.B. and M.W. acknowledges the support of the BMBF collaborative project MUSIKA. E.V. acknowledges the support by NSF grant DMS-1304211. We thank Shmuel Rubinstein for insightful discussions about our paper folding experiments.

- [1] M. Schenk, S. G. Kerr, A. M. Smyth, and S. D. Guest, in *Proceedings of the First Conference Transformables 2013*, September (2013).
- [2] J. L. Silverberg, A. A. Evans, L. McLeod, R. C. Hayward, T. C. Hull, C. D. Santangelo, and I. Cohen, *Science* **345**, 647 (2014).
- [3] T. Tachi, in *Symposium of the International Association For Shell And Spatial Structures (2009)* (2009).
- [4] Y. Yoshimura, *On the Mechanism of Buckling of a Circular Cylindrical Shell Under Axial Compression*, Tech. Rep. (National Advisory Committee for Aeronautics, Washington, 1955).
- [5] A. P. Coppa, *AIAA Journal* **5**, 750 (1967).
- [6] S. D. Guest and S. Pellegrino, *Journal of Applied Mechanics* **61**, 773 (1994).

- [7] H. Yasuda and J. Yang, *Physical Review Letters* **114**, 185502 (2015).
- [8] A. L. Cauchy, *Journal de l'Ecole Polytechnique* **9**, 68 (1813).
- [9] R. Connelly, *Mathematics Magazine* **52**, 275 (1979).
- [10] R. Connelly, I. Sabitov, and A. Walz, *Beiträge zur Algebra und Geometrie* **38**, 1 (1997).
- [11] We refer to the supplementary material for a precise definition of what we mean by “piecewise C^4 ” in this case.
- [12] W. S. Massey, *Tohoku Mathematical Journal, Second Series* **14**, 73 (1962).

APPENDIX: SUPPLEMENTARY MATERIAL

On the regularity of the origami's embedding

Here we make precise the regularity of the function f that maps the flat material domain with fold lines to the 3D origami cylinder. In order to define the domain of f , first remove the (finite number of) fold lines from the material domain. Now consider the topological closure of the resulting set such that fold lines are doubled—with the two copies of each original fold line only identified at their endpoints. I.e., the new domain is a planar rectangle whose boundary consists of the original material boundary and two distinct line segments for each original fold line. We require f to be a C^4 -isometry (up to and including the boundary) on this new domain. By our requirements, fold lines get mapped to straight line segments; hence, the two copies of each original fold line must occupy the same position in space. Notice that a C^4 -isometry (up to and including the boundary) excludes cone points.

Flatness of facets

Let facets denote those connected components of the origami cylinder that arise when all folds are removed. Internal facets are those that do not meet either of the cylinder's boundaries except at isolated vertices.

Internal facets

Our requirements imply that internal facets must be flat:

Lemma 1. *Let P be a closed non-intersecting polygon with finitely many corners in the plane, which is embedded isometrically via a C^4 map f into \mathbb{R}^3 such that each boundary edge of P is mapped to a straight line segment in \mathbb{R}^3 . Then the resulting surface S is contained in a plane.*

Proof. Since S is developable, its Gauß curvature vanishes everywhere. Let parabolic points be those points of S with nonvanishing mean curvature and call all other points flat. Asymptotic curves are those curves in S whose tangent vectors coincide with directions of vanishing directional curvature. Notice that through each parabolic point there exists a unique (up to reparameterization and extension) asymptotic curve. We require the following two facts about developable C^4 surfaces [12]:

- (i) Every asymptotic curve that originates in a parabolic point cannot contain flat points.
- (ii) If an asymptotic curve contains a parabolic point, then it is a straight line segment.

Suppose that S contained a parabolic point. By continuity of curvature, the set of parabolic points is open in S , so there exists a curve Γ of nonzero arc length in S that consists entirely of parabolic points and that intersects asymptotic curves transversally. Then (i) and (ii) imply that S contains a family of straight line segments (consisting entirely of parabolic points), originating from each point of Γ . Each of these line segments intersect the boundary of S in (at least) two different points which vary continuously with their origin on Γ . Since not both of these intersections can be constant along Γ (if they were, then all asymptotic curves would be the same, thereby contradicting the fact that Γ is transversal and has nonzero length), there exists a point on Γ whose asymptotic line meets the boundary of S transversally at a point that is not a corner. But then this point of intersection contradicts (i) since it is flat. Hence S consists entirely of flat points. \square

In order to treat the remaining facets, i.e., those that meet the origami cylinder's boundary, we require a property about the reconstruc-

tion of developable ruled surfaces from maximal geodesics that are transversal to rulings.

Reconstruction of a developable surface from a known geodesic

We call a ruled surface S generated by a *directrix curve* γ (with $|\dot{\gamma}(t)| = 1$ for all t) and a *director curve* v (with $|v(t)| = 1$ for all t) if S is given by $\{\gamma(t) + sv(t)\}$.

Theorem 1. *Let S, \tilde{S} be C^3 developable ruled surfaces that are generated by a directrix curve γ and two director curves v, \tilde{v} . If $\ddot{\gamma}(t) \neq 0$ for all t and γ is a geodesic in both S and \tilde{S} then v and \tilde{v} must agree up to sign.*

Proof. The surface S can be parameterized via $f(s, t) = \gamma(t) + sv(t)$. From the fact that γ is a geodesic, it follows that $\ddot{\gamma}$ is normal to S . Let $N := \ddot{\gamma}/|\ddot{\gamma}|$. Notice that $N(t)$ is normal to S along the ruling $\{\gamma(t) + sv(t)\}$. The ruling direction is obviously a tangent direction of S , so that

$$v = \cos \varphi \cdot \dot{\gamma} + \sin \varphi \cdot (N \times \dot{\gamma}) \quad (2)$$

with an angle function φ .

The second fundamental form of S is given by

$$\text{II} = \begin{pmatrix} \langle f_{tt}, N \rangle & \langle f_{st}, N \rangle \\ \langle f_{ts}, N \rangle & \langle f_{ss}, N \rangle \end{pmatrix}.$$

Developability implies that the determinant of II vanishes on an open and dense subset of S . Since f_{ss} is zero, we conclude that the off-diagonal entries of II must also be zero. Hence, the vector $f_{st} = \dot{v}$ is perpendicular to the surface normal.

Taking derivatives of Equation (2) with respect to t gives

$$\begin{aligned} \dot{v} &= -\dot{\varphi} \sin \varphi \cdot \dot{\gamma} + \cos \varphi \cdot \ddot{\gamma} + \\ &\quad \dot{\varphi} \cos \varphi \cdot (N \times \dot{\gamma}) + \\ &\quad \sin \varphi \cdot (\dot{N} \times \dot{\gamma} + N \times \ddot{\gamma}). \end{aligned}$$

We have $N \times \ddot{\gamma} = 0$ since N is parallel to $\ddot{\gamma}$. Furthermore, the component of \dot{v} along the surface normal must vanish:

$$0 = \cos \varphi \langle \ddot{\gamma}, N \rangle + \sin \varphi \langle \dot{N} \times \dot{\gamma}, N \rangle.$$

To deal with the first term, notice that $\langle \dot{\gamma}, N \rangle = 0$, which implies that we have $\langle \ddot{\gamma}, N \rangle + \langle \dot{\gamma}, \dot{N} \rangle = 0$. This turns the above equation into

$$0 = \cos \varphi \langle \dot{\gamma}, \dot{N} \rangle + \sin \varphi \langle \dot{\gamma} \times \dot{N}, N \rangle.$$

Since $\ddot{\gamma}(t) \neq 0$, the angle $\psi := \angle(\dot{N}, \dot{\gamma})$ can be obtained from γ alone. Hence, the above equation turns into

$$\begin{aligned} 0 &= \cos \varphi \cos \psi + \sin \varphi \sin \psi \\ \Leftrightarrow 0 &= \cos(\varphi - \psi). \end{aligned}$$

From the knowledge of ψ we can infer φ , which, together with N , uniquely determines v . \square

Boundary facets

Even though our origami cylinder only contains line segments as fold lines, it is not a priori clear that the cylinder's boundaries are also polygonal lines. In this section, we show that they must nevertheless be piecewise straight if the cylinder's embedded height is strictly smaller than the material height h . In any case, we have already shown that facets which are completely enclosed by fold lines must be flat. We now extend this result to those facets that meet the cylinder's boundary.

Theorem 2. *Every origami cylinder whose height is strictly less than the material height consists entirely of planar facets.*

Proof. For a given origami cylinder whose embedded height is (strictly) less than the material height, consider a segment of either boundary that is at least C^4 (i.e., does not contain vertices). Let γ and Γ be the corresponding material and embedded curves of such a boundary segment, and assume, by contradiction, that Γ

is curved (i.e., its second derivative is nowhere zero—this can always be achieved by restriction to a part of the segment). Since Γ consists entirely of parabolic points, each point carries a unique asymptotic line, whose collection is a ruled developable surface to which we apply the previous theorem.

By our definition of origami cylinders, Γ lies in a horizontal plane and thus satisfies $\psi \equiv 0$, implying $\varphi \equiv \frac{\pi}{2}$, where ψ and φ refer to the angle functions in the proof of Theorem 1. This and the fact that the curvature vector of Γ is parallel to the (xy) -plane imply that the asymptotic lines emanating from Γ are strictly vertical. By property (i) above, these asymptotic lines cannot contain flat points and thus cannot meet fold lines transversally. Since the number of fold lines is finite, this implies that there exists an asymptotic line that traverses the cylinder from top to bottom. But then the cylinder's height equals the material height, contradicting the initial assumption. \square

Fan structure

In this section we analyze properties of individual fans. Denote by h a fan's material height and by $H < h$ its embedded height. Denote by a the fan's top vertex in the material domain, and let A be its embedded position. Likewise, let p_1, \dots, p_n be the bottom vertices in the material domain, and denote the attendant spatial points by P_1, \dots, P_n , which we suppose to lie in the (xy) -plane. By the previous discussions on flatness of facets, we know that the embedded fan's boundary must be a polygonal line whose corners are a subset of the P_i (since folds might have zero dihedral angle) and that its faces must be flat triangles.

Construction of fans from given boundary vertices

Suppose that the apex vertices a and A and the boundary vertices p_1, p_n and P_1, P_n of a

fan are given in the material and spatial domain, respectively. Below we offer a construction for the interior vertices p_2, p_3, \dots, p_{n-1} and P_2, P_3, \dots, P_{n-1} such that the resulting embedding is isometric. For this construction to work, the *only* condition to be met is that $|P_n P_1| \leq |p_n p_1|$ as shown by the following result.

Theorem 3. *Consider a triangle $\Delta(abc)$ in the plane and a triangle $\Delta(ABC)$ in \mathbb{R}^3 . Let E be any plane containing B and C . If the following conditions are satisfied*

- $|AB| = |ab|$,
- $|AC| = |ac|$,
- $|BC| \leq |bc|$,
- $H \leq h$, where H is the distance from A to the plane E and h is the distance from a to bc ,

then there exists a point D on E such that the triangle pair $\Delta(ABD) \cup \Delta(ADC)$ is isometric to $\Delta(abc)$.

Proof. Consider the set of all points $D \in E$ with $|BD| + |DC| = |bc|$. This locus of points forms an ellipse η in the plane E with foci B and C . It suffices to show that for some D on this ellipse, $\angle BDA + \angle ADC = \pi$, for if this is the case, then the hinge composed of the two triangles $\Delta(ABD)$ and $\Delta(ADC)$ can be isometrically unfolded into a triangle congruent to $\Delta(abc)$.

Let \bar{A} be the orthogonal projection of A onto E . First, \bar{A} lies on or outside of the ellipse η :

$$\begin{aligned} |\bar{A}B| + |\bar{A}C| &= \\ &= \sqrt{|AB|^2 - H^2} + \sqrt{|AC|^2 - H^2} \\ &= \sqrt{|ab|^2 - H^2} + \sqrt{|ac|^2 - H^2} \\ &\geq \sqrt{|ab|^2 - h^2} + \sqrt{|ac|^2 - h^2} \\ &\geq |bc|, \end{aligned}$$

precisely the condition that \bar{A} does not lie inside η .

Now consider the angle bisector of the angle $\angle B\bar{A}C$, and denote its two intersection points

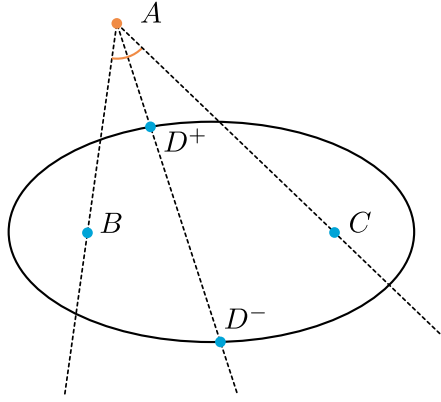


Figure 6: On the ellipse with foci B and C , the points D^+ and D^- lie on the intersection of the ellipse with the angular bisector of the angle $\angle B\bar{A}C$.

with η by D^+ and D^- , where D^+ is closer to \bar{A} , see Figure 6. Then

$$\begin{aligned}\angle BD^+A + \angle AD^+C &\geq \pi, \\ \angle BD^-A + \angle AD^-C &\leq \pi.\end{aligned}$$

In order to prove, e.g., the first line, express the cosine of the two angles via the inner product of the vectors $(B - D^+)$, $(C - D^+)$, and $(A - D^+)$:

$$\begin{aligned}\cos \angle BD^+A &= \frac{\langle B - D^+, A - D^+ \rangle}{|B - D^+| |A - D^+|} = \frac{1}{|A - D^+|}, \\ \cos \angle AD^+C &= \frac{\langle C - D^+, A - D^+ \rangle}{|C - D^+| |A - D^+|} = \frac{1}{|A - D^+|}.\end{aligned}$$

Since $(B - D^+)$ and $(C - D^+)$ are horizontal, the only quantity that depends on H is the length $|A - D^+|$. We leverage this fact to conclude that the cosines' sign is independent of H . For the sake of brevity, write

$$\begin{aligned}\cos \angle BD^+A &= \frac{c_1}{\sqrt{c_3^2 + H^2}}, \\ \cos \angle AD^+C &= \frac{c_2}{\sqrt{c_3^2 + H^2}}.\end{aligned}$$

Proving that $\angle BD^+A + \angle AD^+C \geq \pi$ is equivalent to proving that

$$\sin(\angle BD^+A + \angle AD^+C) \leq 0$$

since $\angle BD^+A + \angle AD^+C < 2\pi$ by construction. Since each individual angle is bounded above by π , we use $\sin(x) = \sqrt{1 - \cos(x)^2}$ to obtain

$$\begin{aligned}\sin(\angle BD^+A + \angle AD^+C) &= \\ \frac{\left(c_2 \sqrt{c_3^2 - c_1^2 + H^2} + c_1 \sqrt{c_3^2 - c_2^2 + H^2} \right)}{c_3^2 + H^2}.\end{aligned} \quad (3)$$

To show that this expression is nonpositive, we show that it either vanishes for all H or that it is negative for $H = 0$ and cannot vanish for any other H in this case. Continuity then implies the desired conclusion.

It is straightforward to verify (using the Cauchy-Schwarz inequality) that $c_3^2 \geq c_1^2$ and $c_3^2 \geq c_2^2$. Hence, if the expression in (3) is zero for some H_0 , then either both c_1 and c_2 are zero or both are nonzero with different sign. If both are zero, then both angles $\angle BD^+A$ and $\angle AD^+C$ are equal to $\pi/2$ regardless of H and the expression in (3) vanishes for all H . If both are nonzero, rearranging terms in (3) yields $c_1 + c_2 = 0$, which is equivalent to $\angle BD^+A = \pi - \angle AD^+C$. This holds independently of H , so again the expression in (3) vanishes for all H .

Hence, the expression in (3) either vanishes for all H or does not vanish for any H . In the former case, there is nothing to show. Consider the latter case and let $H = 0$. Then A and \bar{A} agree and D^+ lies in the inside or on the boundary of the triangle $\Delta(ABC)$, which necessitates $\angle BD^+A + \angle AD^+C \geq \pi$ with equality if and only if the expression in (3) vanishes, which we have ruled out by assumption.

In order to finish the proof of Theorem 3, notice that $\angle BDA + \angle ADC$ is continuous as D sweeps along an arc of the ellipse between D^- and D^+ ; hence, there must exist a D with $\angle BDA + \angle ADC = \pi$. \square

Remark 1. There are at least two distinct such points $D \in E$ unless the ellipse is degenerate or \bar{A} lies on η , which occurs when one of the inequalities in the theorem statement becomes tight: $|BC| = |bc|$ or $H = h$. In Figure 4, the

two solutions are the points F and G (see below for an explanation).

The previous theorem shows that as soon as A , P_1 , and P_n have been placed in such a way that $|P_1P_n| \leq |p_1p_n|$, it is always sufficient to introduce a single interior fold to obtain a valid isometric embedding of the material triangle AP_1P_n . This, together with the following lemma, provides a method of constructing fans with an arbitrary (but still finite) number of interior folds.

Lemma 2. *Denote by \bar{A} the vertical projection of A onto the (xy) -plane. Then the angle $\varphi_i = \angle \bar{A}P_iP_{i+1}$ satisfies*

$$\cos(\varphi_i) = \frac{-u_i}{\sqrt{h^2 - H^2 + u_i^2}}, \quad (1)$$

where u_i is the signed horizontal distance in the material from a to p_i , see Figure 4.

Proof. Choose coordinates in the (xy) -plane such that $P_i = (0, 0)$ and \bar{A} lies along the x -axis, i.e., $\bar{A} = (\sqrt{h^2 - H^2 + u_i^2}, 0)$. The next point P_{i+1} will be at (x, y) , where x and y have yet to be found. Two length constraints have to be satisfied:

$$\begin{cases} |P_iP_{i+1}|^2 = (u_{i+1} - u_i)^2, \\ |P_{i+1}\bar{A}|^2 = h^2 - H^2 + u_{i+1}^2. \end{cases}$$

Algebraic manipulation gives that

$$\begin{cases} x = (u_{i+1} - u_i) \frac{-u_i}{\sqrt{h^2 - H^2 + u_i^2}} \text{ and} \\ y = (u_{i+1} - u_i) \frac{\pm\sqrt{h^2 - H^2}}{\sqrt{h^2 - H^2 + u_i^2}} \end{cases},$$

which proves our claim. \square

Using this lemma, notice that P_2 lies on one of two rays originating at P_1 which enclose an angle of $\pm\varphi_1$ with the line $P_1\bar{A}$. Once one of the rays is chosen, consider the ellipse η given by the set $\{P : |P_1P| + |PP_n| = |p_1p_n|\}$ and place P_2 at any point on the chosen ray inside η . As an illustration, P_2 can be placed at any point that lies on one of the bold line segments P_1F and

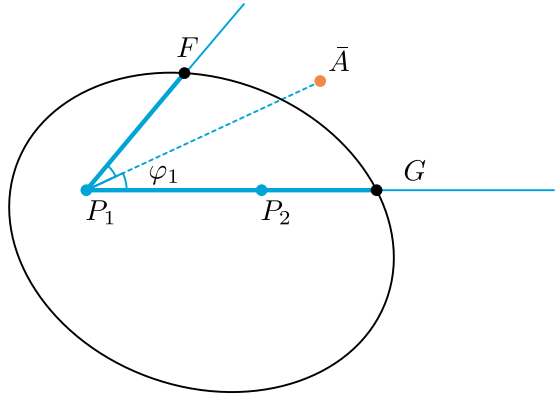


Figure 7: Illustration of the construction of P_2 . The points F and G arise from the intersection of the two rays emanating from P_1 with the ellipse.

P_1G in Figure 7. Notice that by assumption $|P_1P_n| \leq |p_1p_n|$, which implies that

$$\begin{aligned} |P_2P_n| &\leq |p_1p_n| - |P_1P_2| \\ &= |p_1p_n| - |p_1p_2| \\ &= |p_2p_n|. \end{aligned}$$

Consequently, the conditions of Theorem 3 are satisfied for all i with $A = A$, $B = P_i$, $C = P_n$, $a = a$, $b = p_i$, and $c = p_n$ and the construction that lead to P_2 can now be repeated for P_3 and so forth.

The statement of Theorem 3 then has two consequences: (a) If we place P_i on the attendant ellipse during our construction, then P_i corresponds to one of the points D from the theorem and all subsequent vertices P_{i+1}, \dots, P_n lie on a straight line. (b) If, on the other hand, we place P_2, P_3, \dots, P_{n-2} strictly *inside* the attendant ellipses, then the existence of the point D of the theorem guarantees that we can always construct the penultimate vertex P_{n-1} to obtain an isometric embedding.

Remark 2. Similarly, one can consider a more general (and more symmetric) variant of the above construction, by first placing the vertices P_2, P_3, \dots, P_i , then $P_{n-1}, P_{n-2}, \dots, P_{n-k}$, then

placing $P_{i+1}, P_{i+2}, \dots, P_{i+j}$, and so forth, i.e., by alternating the placement of new vertices between left and right, until all vertices have been placed. Indeed, if P_{i+1} and P_i are given, P_{i-1} can be found on the ray obtained by rotating the line $P_i\bar{A}$ about P_i by an angle of $\tilde{\varphi}_i$ in either direction, where

$$\cos \tilde{\varphi}_i = \frac{u_i}{\sqrt{h^2 - H^2 + u_i^2}}.$$

Notice that the only difference to Equation (1) is the different sign of the right-hand side. A similar argument as above then guarantees that the result is an isometric embedding.

We fix the following notation:

Definition. Let φ_i be as in Eq. (1). We call $\{P : \angle PP_i\bar{A} = \pm\varphi_i\}$ and $\{P : \angle PP_i\bar{A} = \pm\tilde{\varphi}_i\}$ the forward and backward rays emanating from P_i , respectively.

Remark 3. A consistency check is to consider the case where $h = H$, i.e., the case of finding a completely uncompressed embedding for an entire strip. Assuming the absence of vertical folds (which correspond to $u_i = 0$ and would allow for embedding the paper as a prism), we expect the only possible embedding of the strip to be the flat embedding (which of course violates our definition of an origami cylinder since it is not a cylinder in the topological sense). This is reflected by Equation (1), which implies that $\cos \varphi_i = \pm 1$, resulting in turning angles of $2\varphi_i = 2\pi k$, $k \in \mathbb{Z}$.

Embedding a given fold pattern

So far, we have considered the problem of finding positions for interior vertices p_2, \dots, p_{n-1} and P_2, \dots, P_{n-1} simultaneously under the assumption that a fan's boundary vertices are given. We now turn to the question of constructing P_2, \dots, P_{n-1} under the additional assumption that p_2, \dots, p_{n-1} are given in the material domain, i.e., under the assumption of a given fold pattern. Then the construction of the previous section can in principle be

repeated—with the additional restriction that P_{i+1} must be located at distance $|p_{i+1} - p_i|$ from P_i on one of the forward rays from P_i . Additionally, one or both of the resulting positions for P_{i+1} might lie outside the attendant ellipse with foci P_i and P_n , which poses additional restrictions. Indeed, a given fold pattern is isometrically realizable if in each of the above construction steps, the new vertex P_{i+1} lies on the forward rays from P_i and inside or on the corresponding ellipse, and the last point, P_{n-1} , resides on the respective ellipse. Finding a valid embedding thus requires to test for up to 2^{n-2} possible choices for placing (P_2, \dots, P_{n-1}) .

Notice that there is no a priori guarantee that a given fold pattern is isometrically embeddable. However, if there is a configuration where P_2, \dots, P_{n-1} lie strictly inside their respective ellipses and, in particular, P_{n-1} does not lie on its corresponding ellipse, then our construction implies that there exists a material point between p_{n-1} and p_n such that if we insert an extra fold line from a to this point, then the resulting pattern is indeed isometrically embeddable.

Fold pattern validity

The previous discussion can be turned into an algorithm for testing whether or not a given fold pattern can be isometrically embedded as an origami cylinder. To this end, suppose that a fold pattern and the heights for each individual strip of this pattern are prescribed. Then:

1. Divide the pattern into strips and proceed strip-wise. Notice that the newly introduced horizontal fold lines that demarcate the strips' boundaries are auxiliary and must consequently have vanishing dihedral angles (see below).
2. Divide each strip into fans, proceed fan-wise. Quadrilateral surface pieces are split into triangles by adding another auxiliary diagonal fold line.

3. Using the above notation, embed each fan by first placing P_1 and iteratively constructing the 2^{n-1} total positions of P_2, \dots, P_n by placing P_{i+1} on each of the two possible forward rays emanating from P_i at the distance prescribed by the given fold pattern. Since P_n is no longer prescribed, all embeddings are valid isometric embeddings of the single fan.
4. Concatenate all fans and check if there is a possible embedding of the current strip that closes up.
5. Stack the individual embedded strips to obtain the origami cylinder. Here, adding a new strip to the stack requires finding an embedding for a given material strip with the additional constraint that one boundary of the strip is prescribed. Notice that, even if the strip is embeddable with this additional constraint, there is no guarantee that the auxiliary folds that are introduced by dividing the material into strips have vanishing dihedral angle, which is an extra condition to be met.

Calculating the zeros of the so-called *gap function* (see below) leads to an extension of this algorithm to the case where just the fold pattern is prescribed *without* additionally prescribing the heights of individual strips.

Turning angles between consecutive fans

Recall that in an isometric embedding of a strip, upward and downward fans alternate. Denote, as above, by A the apex of a downward fan, and let A_0 and A_2 be the vertices adjacent to A on the strip's upper boundary, and let P_1, \dots, P_n be the vertices of the fan with apex A on the strip's lower boundary. In this section we establish a relationship between the angle $\alpha = \pi - \angle A_0 A A_2$ on the strip's upper boundary and the (alternating) sum of turning angles $2\varphi_i = \pm(\pi - \angle P_{i-1} P_i P_{i+1})$ along the

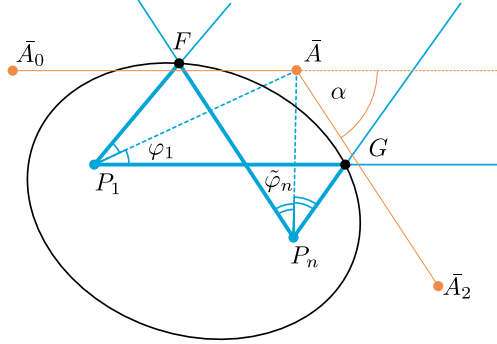


Figure 8: Illustration of the angle α on the strip's upper boundary and the angles φ_i along the fan's lower boundary. F and G denote the intersections of the forward rays emanating from P_1 and backward rays emanating from P_n .

fan's lower boundary, which can be computed using Lemma 2. Notice that Lemma 2 implies that there are two choices for the line segment $P_i P_{i+1}$: it must lie on one of the two forward rays originating at P_i enclosing an angle of $2\varphi_i$, placed such that the line $P_i \bar{A}$ is the angular bisector. Since it is always possible to embed isometrically with zero turning angle at P_i (if the fold from A to P_i has zero dihedral angle), one of those rays must be the continuation of the line segment $P_{i-1} P_i$. Thus, the turning angle of the lower boundary at the vertex P_i is either 0 or $\pm 2\varphi_i$. From now on we discard the vertices P_i that have zero turning angle in all notation and all formulas.

In order to establish a relationship between α and the angles φ_i , observe that the line segment $A_0 A$ must be parallel to one of the forward rays originating from P_1 which contain P_2 and that similarly the line segment $A A_2$ must be parallel to one of the backward rays from P_n containing P_{n-1} (see Figure 8). In order to illustrate the relationship between α and the angles φ_i , consider the case $n = 3$. With reference to Figure 8, P_2 must in this case coincide with either F or G . If $P_2 = F$, then $\alpha = 2\varphi_1 - 2\varphi_2$, while $\alpha = 2\varphi_2 + 2\varphi_3$ if $P_2 = G$, see Figure 9. For the

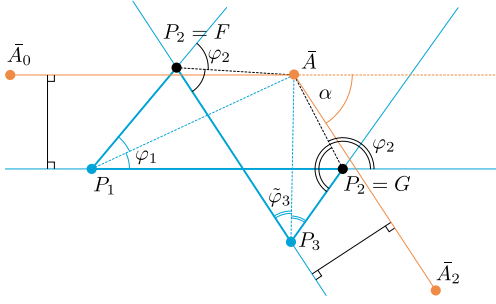


Figure 9: Illustration of the angles φ_2 and the relation to α for the different choices of P_2 in the case $n = 3$. Notice that α refers to the signed angle while the φ_i and $\tilde{\varphi}_i$ defined via (1) are unsigned.

general case of arbitrary $n \geq 3$, let

$$S := \sum_{i=2}^{n-1} (-1)^i 2\varphi_i.$$

Then, depending on the parity of n and the two possible choices for placing P_2 , one obtains the following table:

	n even	n odd
$P_2 \in P_1 F$	$\alpha = -S + 2\varphi_1 + 2\tilde{\varphi}_n$	$\alpha = -S + 2\varphi_1$
$P_2 \in P_1 G$	$\alpha = S$	$\alpha = S + 2\tilde{\varphi}_n$

Notice that the choice of forward rays for P_2 together with the parity of n directly determines which backward ray from P_n contains P_{n-1} as all P_i must now have nonzero turning angles.

The boundary gap function

We now turn to the question of compressibility. Our main result is:

Theorem 4. *An origami cylinder whose fold pattern does not contain vertical fold lines has at most a finite number of heights at which its fold pattern can be isometrically embedded. Hence, isometric deformations with continuously varying heights are impossible in this case.*

Proof. Consider a single strip. A necessary condition for the existence of an embedding at a given height H is that the strip closes up into a cylinder. Our construction above provides a method for constructing isometric embeddings of a strip starting at a boundary vertex P_0 of a strip's fan with respective material point p_0 . After the embedding is completed, p_0 might be located at two different spatial positions Q_0 and P_0 . The *gap function* is defined as $g := |Q_0 - P_0|^2$ and is a function of H alone (see below). The gap function may depend on the choice of p_0 and can also differ between the two boundaries of a strip; any choice of P_0 suffices for our purpose. For the strip to be isometrically embeddable as an origami cylinder at a certain height H , it is necessary for g to have a zero at H . Likewise, if the embedded strip were continuously deformable between H_0 to H_1 , then g would have to vanish on the entire interval $[H_0, H_1]$. We show that this is impossible.

Explicitly, g can be expressed by adding the boundary's individual line segments. Let l_i be the i -th segment's length and denote by ψ_i its total argument. Then

$$g = \left| \sum_{i=1}^N l_i (\cos \psi_i, \sin \psi_i) \right|^2. \quad (4)$$

With regards to the notation of the previous section, the angles ψ_i can be expressed (up to a constant offset) by adding all individual turning angles up until the i -th line segment. Since the individual turning angles at each turning point are known to be $\pm 2\varphi_i$ for interior vertices and either of $\{0, \pm 2\tilde{\varphi}_n, \pm 2\varphi_n, \pm (2\varphi_n + 2\tilde{\varphi}_n)\}$ for vertices on a fan's boundary—and all φ_i and $\tilde{\varphi}_i$ are known from Lemma 2—we obtain an explicit expression of g as a function only of the embedded height H . This applies to both upward and downward fans in the strip since a fan's top and bottom turning angles are related according to the previous section.

It now follows from Equation (4) that g is a combination of functions that are analytic in

H (the ψ_i are since the φ_i are while the l_i are constants) and thus g is analytic in H . Furthermore, according to Remark 3, if $H = h$, then the φ_i are integer multiples of π (since all u_i are nonzero by assumption). Accordingly, for

$H = h$, the angles ψ_i must be integer multiples of 2π and hence $g(H = h)$ is equal to the material width w . This means that g cannot be the zero function and must therefore have isolated zeros. \square